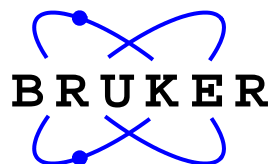


# RF GRASP™

## NMR Spectroscopy with Radio Frequency Gradients.



**Werner E. Maas**  
Bruker Instruments, Inc.  
19 Fortune Drive  
Billerica, MA 01821 USA

version 1.2  
February, 1996

Copyright 1996 Bruker Instruments, Inc.  
P/N B1161

# Warning

**THE RF GRASP™ ACCESSORY OPERATES WITH HIGH VOLTAGES. ALWAYS DISCONNECT THE POWER CORD FROM THE RF CHANNEL SELECTOR UNIT BEFORE OPENING THE PROBE, THE RF CHANNEL SELECTOR OR THE RF DUPLEXER**

**Copyright 1996 Bruker Instruments, Inc.**

The information contained in this manual may be altered without notice. Bruker accepts no responsibility for actions taken as a result of the use of this manual. Bruker accepts no liability for any mistakes contained in the manual, leading to coincidental damage, whether during installation or operation of the instrument. Unauthorized reproduction of manual contents, without written permission from the publishers, or translation into another language, either in full or in part, is forbidden.

## Table of Contents

1	Introduction .....	4
2	Geometry of the RF Gradient Field .....	5
3	Design of the RF GRASP™ probe .....	5
4	Spin Dynamics .....	6
4.1	Hamiltonians .....	6
4.2	Gradient Conversion Cycles .....	7
4.3	Coherence Orders .....	8
5	Radiation Damping .....	9
6	Experiments with the RF GRASP™ probe .....	10
6.1	Experimental Set-Up .....	10
6.2	Calibration of the RF Gradient .....	12
6.3	P/N type Cosy selection .....	14
6.4	Double Quantum filtered Cosy .....	16
6.5	Solvent suppression with RF gradients .....	18
6.6	Heteronuclear Single Quantum Correlation .....	20
7	References .....	22
8	Appendix .....	23
8.1	Definitions for gradient switching .....	23
8.2	Gradient conversion cycle .....	23
8.3	rfg.nutation .....	23
8.4	rfg.cosy .....	24
8.5	rfg.dqfcosy .....	26
8.6	rfg.watersup .....	27
8.7	rfg.hsqc .....	28

# 1 Introduction

Gradients have been shown to be extremely useful for coherence selection in high resolution NMR. The use of gradients to dephase unwanted coherences prior to acquisition leads to an increase in dynamic range, as compared to the traditional phase cycling methods.

Whereas  $B_0$  or DC gradients are the most commonly employed gradient fields, RF or  $B_1$  gradients are not new, but their application has been limited to the residual inhomogeneity of nominally homogeneous RF coils. These gradients are very useful, but their strength is limited since the coils are optimized for a homogeneous RF field. Stronger gradients can be obtained using specially designed RF coils and recently the use of a separate RF gradient coil, in addition to a homogeneous RF coil has been introduced<sup>1-3</sup>.

A reason for investigating  $B_1$  gradients is that RF gradients offer some advantages over DC gradients, such as:

- short switching times
- no eddy currents are induced
- frequency selective, either for a given nucleus or for a specific resonance
- no need for preemphasis

Both types of gradient fields, however, differ markedly in their interaction with the spin system.

**$B_0$  gradients** are *secular* and therefore:

- can not induce coherence transformations
- couple into the spin system via  $I_z$
- are always orthogonal to transverse magnetization
- the spin dynamics are independent of the gradient coil geometry.

On the other hand **RF gradients** are *non-secular* and therefore

- can induce coherence transformations
- couple into the spin system from anywhere in the transverse plane
- the spin dynamics are very dependent of the gradient coil geometry
- the orthogonality condition is only met if the gradient coil and the homogeneous coil are the same.

## 2 Geometry of the RF Gradient Field

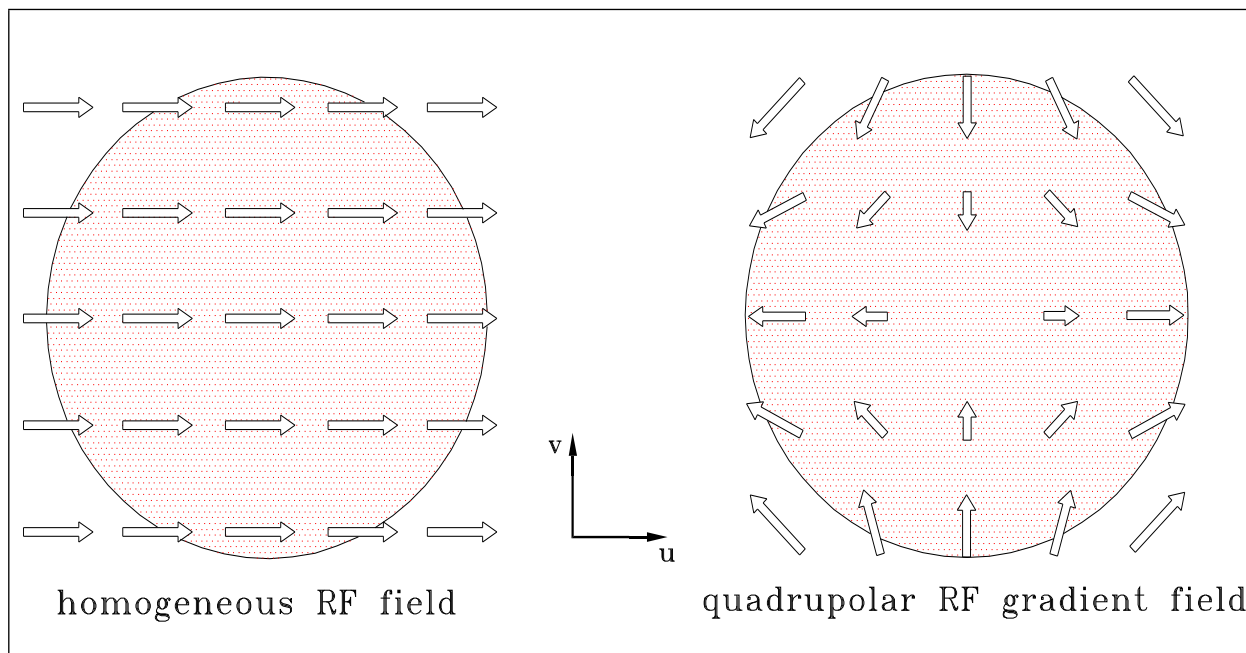


**Figure 1** *Geometry of the RF fields generated by a homogeneous coil and a quadrupolar coil, related to the laboratory axes  $u$  and  $v$ .*

The spatial variation of the RF gradient field can, by design, be contained in the amplitude of the field or in the phase of the field or in both simultaneously. In the case of a *planar* gradient field the amplitude of the RF field is spatially dependent, while the phase is constant. The residual inhomogeneity of a homogeneous RF coil is a perfectly planar gradient, since the gradient and homogeneous RF are generated by one and the same coil. An RF gradient in which only the phase varies over space is used in radial spectroscopy<sup>4</sup>.

In our approach to RF gradient spectroscopy we have used a quadrupolar RF coil. The field generated by a quadrupolar coil has a spatially dependent phase and amplitude which vary in the transverse plane and are constant along the  $z$ -direction. The RF amplitude is zero in the center of the transverse plane and increases with increasing radius, while the phase at constant radius varies over  $2\pi$  (see Figure 1). The quadrupolar coil design is chosen because it optimizes RF efficiency and filling factor and it generates the maximum gradient strength.

## 3 Design of the RF GRASP™ probe

The Bruker RF GRASP™ is equipped with both a homogeneous  $^1\text{H}$  RF coil and a quadrupolar gradient  $^1\text{H}$  RF coil. The probe is similar to an inverse detection probe, but the  $^2\text{D}$  lock will appear weaker than one is accustomed to using conventional probes. As a result one may have to use higher values for the lock power than usual. Problems with locking are anticipated when using small amounts of lock substance or when the magnetic field is inhomogeneous. It is therefore

suggested to shim the probe while locking on a strong deuterium signal (such as at least 50% D<sub>2</sub>O or 50% D-acetone) before attempting to lock on less sensitive samples.

The homogeneous and gradient RF coils are electrically isolated via an active switching mechanism. The coil switching is driven by the RF-Channel Selector™, which is controlled from the pulse program via a control signal. By convention **NMRword8 bit 7** is used to switch the probe between the gradient mode and the homogeneous mode. In the normal state (*CH1 high*, light on) the homogeneous coil is active and the gradient coil is turned off. By changing the status of the nmrword from the pulse programmer (see appendix and the experimental section) the gradient coil is activated (*CH2 high*) and the homogeneous coil is switched off.

RF is delivered to both coils via separate inputs on the probe. The RF power can be generated from two different amplifiers or it can be derived from a single amplifier by using the **RF GRASP™-Duplexer**. The Duplexer has a single RF input port and two RF output ports, one for each proton channel on the probe. In normal operation (*CH1 and CH3 high*) the RF power is routed to RF output 1 (*RF OUT1*) on the duplexer, which should be connected to the homogeneous RF coil via the preamp. Upon switching the probe to the RF gradient channel (*CH2 and CH4 high*) the duplexer switches the RF power to *RF OUT2*, which is connected to the gradient channel on the probe.

## 4 Spin Dynamics

### 4.1 Hamiltonians

The interaction of an RF pulse with phase  $\theta$  on a homogeneous coil with the sample can be described by a Hamiltonian  $H_h$

$$(1) H_h = -\gamma B_{1h}(I_x \cos \theta + I_y \sin \theta)$$

In the case of an x-pulse ( $\theta=0$ ), magnetization perpendicular to the rotating frame x-axis will rotate in the yz-plane and magnetization along the x-axis will remain invariant. The Hamiltonian  $H_g$  for an RF field with phase  $\phi$  and generated by a quadrupolar gradient coil is given by:

$$(2) H_g = -\gamma B_{1g} G_x (I_x \cos \theta + I_y \sin \theta) - \gamma B_{1g} G_y (I_y \cos \theta - I_x \sin \theta)$$

in which the gradient terms of the x and y components are written as  $G_x$  and  $G_y$  respectively and

$$G_i = u \frac{\partial B_i}{\partial u} + v \frac{\partial B_i}{\partial v} \text{ and } i=x,y, \text{ with } u \text{ and } v \text{ the directions of the laboratory frame.}$$

A quadrupolar RF gradient pulse spreads the magnetization over the surface of a sphere rather than dispersing the magnetization in a plane in the case of  $B_0$  or planar  $B_1$  gradient fields. Magnetization starting along the z-axis will thus be completely dephased, whereas magnetization components along the rotating frame x and y-axes will remain partially invariant.

## 4.2 Gradient Conversion Cycles

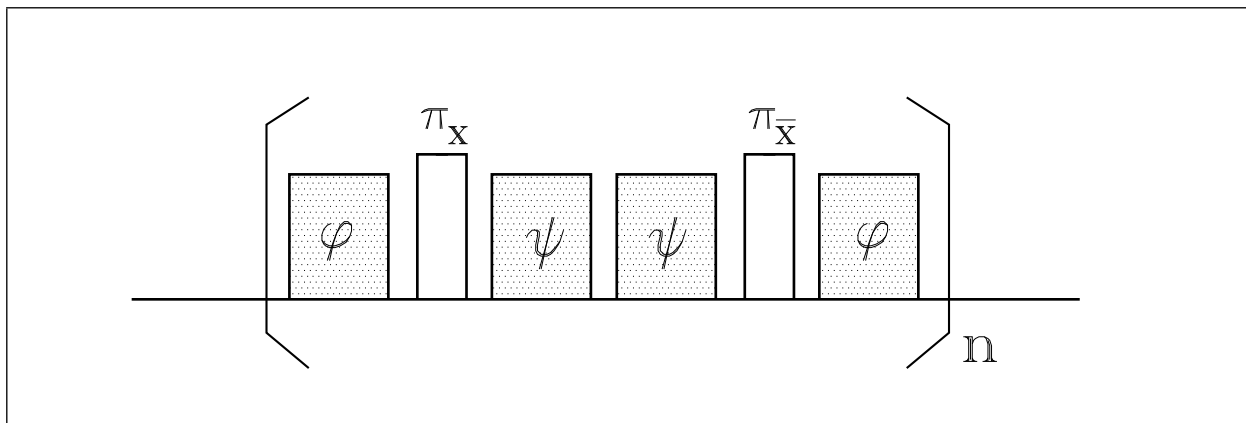


**Figure 2** *Radial to planar gradient conversion cycle, based on  $\pi$  pulses.*

In experiments one sometimes wishes to use a quadrupolar RF gradient while other experiments demand a planar gradient evolution. A quadrupolar RF gradient pulse will by itself dephase all z-components of the magnetization but spin-lock part of the x and y components. Some experiments, such as the solvent suppression sequence<sup>5</sup>, the double quantum filtered COSY experiments<sup>6</sup> and a version of the heteronuclear correlation experiment<sup>7</sup> described below, are designed to use the quadrupolar gradient evolutions as is, by a combination of RF gradient pulses and homogeneous pulses. Other experiments, however, need planar gradient evolutions to eliminate unwanted coherence pathways while retaining a specific coherence.

A planar gradient evolution can be achieved with a quadrupolar gradient coil via so-called *radial-to-planar conversion cycles*<sup>2</sup>. These conversion cycles consist of a string of homogeneous RF pulses, interleaved with periods of gradient evolution. If the gradient evolution is small compared to the nutation by the homogeneous pulses, then the average Hamiltonian adopts the symmetry dictated by the homogeneous pulses.

An example of a conversion cycle which results in a planar gradient evolution is based on homogeneous  $\pi$  pulses:

$$(3) \quad G_{\phi} - \pi_x - G_{\psi} - G_{\psi} - \pi_{\bar{x}} - G_{\phi}$$

where  $G_{\phi}$  and  $G_{\psi}$  are the gradient RF pulses with phases  $\phi$  and  $\psi$ , respectively and  $\pi_x$  and  $\pi_{\bar{x}}$  are the homogeneous RF pulses, with a rotation angle of  $\pi$  radians and phases  $x$  and  $-x$ , respectively. The cycle is diagrammed in Figure 2. The average Hamiltonian for this sequence is:

$$(4) \quad \langle H \rangle = -\gamma B_{1g} \left[ G_x \cos\left(\frac{\phi + \psi}{2}\right) - G_y \sin\left(\frac{\phi + \psi}{2}\right) \right] \\ \left[ I_x \cos\left(\frac{\phi - \psi}{2}\right) + I_y \sin\left(\frac{\phi - \psi}{2}\right) \right]$$

This averaged Hamiltonian is equal to the Hamiltonian for an RF field with phase  $\frac{\phi - \Psi}{2}$  and magnitude  $B_{1g} \sqrt{G_x^2 \cos\left(\frac{\phi + \Psi}{2}\right)^2 - G_y^2 \sin\left(\frac{\phi + \Psi}{2}\right)^2}$ . The phase of the resultant gradient field is no longer dependent on the location in the gradient coil, while the spatial dependence is entirely contained in the magnitude of the resultant field.

This sequence therefore equals a planar gradient which rotating frame phase is determined by the difference of the phases of the quadrupolar gradient pulses and which gradient direction in the lab frame is determined by the sum of the phases of the quadrupolar gradient pulses.

### 4.3 Coherence Orders

<b>z-quantized</b>	<b>x-quantized</b>	<b>y-quantized</b>
$I_z^+ = I_x + iI_y$	$I_x^+ = I_y + iI_z$	$I_y^+ = I_z + iI_x$
$I_z^- = I_x - iI_y$	$I_x^- = I_y - iI_z$	$I_y^- = I_z - iI_x$

**Table 1: Raising and lowering operators quantized along x, y and z.**

In the analysis of  $B_0$  gradient experiments it is common to use the concept of coherence orders. These coherence orders are defined with respect to an  $I_z$  operator and since  $B_0$  gradients are secular and do not induce coherence transformations this concept conveniently deals with this type of gradient fields.

In RF gradient spectroscopy the gradient pulse is responsible for both the dephasing/rephasing and for introducing coherence transformations. This leads to a complex mixture of spinstates due to simultaneous gradient evolution and coherence transformations, but to have a convenient picture of the dynamics it is useful to separate the two operations. One approach to this separation is to quantize the states along the rotating frame axis of the gradient field, so that there are no coherence transformations during the gradient pulse. The re-quantization involves an expansion of the Cartesian single spin operators into raising and lowering operators that are quantized along  $I_x$  and  $I_y$ .

A straight forward expansion of the single spin Cartesian operators leads to the set of raising and lowering operators listed in Table 1. Notice that we have introduced a slight modification to the raising and lowering operator nomenclature to explicitly show the axis of quantization. From Table 1, the effective coherence numbers for the full range of two-spin Cartesian product operators can be calculated for the three axes of quantization, and are shown in Table 2. The details of these redefined coherence orders are described in a publication by Zhang et al.<sup>8</sup>



	$k_x$	$k_y$	$k_z$
$I_x$	0	+/-1	+/-1
$I_y$	+/-1	0	+/-1
$I_z$	+/-1	+/-1	0
$I_x I_x$	0	0,+/-2	0,+/-2
$I_x I_y$	+/-1	+/-1	0,+/-2
$I_x I_z$	+/-1	0,+/-2	+/-1
$I_y I_x$	+/-1	+/-1	0,+/-2
$I_y I_y$	0,+/-2	0	0,+/-2
$I_y I_z$	0,+/-2	+/-1	+/-1
$I_z I_x$	+/-1	0,+/-2	+/-1
$I_z I_y$	0,+/-2	+/-1	+/-1
$I_z I_z$	0,+/-2	0,+/-2	0

Table 2: Effective Coherence Numbers.

## 5 Radiation Damping

Radiation damping is caused by the mutual coupling between a strong NMR signal and the receiver coil. The rotating magnetization induces a current in the receiver coil and in the case of a strong signal this current creates a rotating magnetic field which tilts the magnetization back to its equilibrium position.

The occurrence of radiation damping during non-observation windows in the pulse sequence can be prevented by eliminating the mutual coupling between the sample and the receiver coil. In the **RF GRASP™** probe this is simply done by switching the probe to the gradient channel during free precession delays, which prevents a current to be generated in the homogeneous coil. Although the magnetization can now in principle couple to the RF gradient coil, the magnetization has the wrong symmetry to induce a current in this coil, so that radiation damping is prevented.

Two recent publications<sup>9,10</sup> describe experiments involving Q-switching to avoid radiation damping, using Bruker's new line of **Q-Switch™** probes. Similar results can be obtained with the **RF GRASP™** probe.

## 6 Experiments with the RF GRASP™ probe

In the following sections some examples are given of RF gradient experiments<sup>2,5-8</sup>. The pulse programs for these experiments are given in the appendix. Further experiments involving RF gradients are described in publications by Canet et al.<sup>11-14</sup>, Keeler et al.<sup>1,15,16</sup> and Eads<sup>17</sup>.

### 6.1 Experimental Set-Up

The set-up of the RF GRASP™ accessory is shown schematically in Figure 3. **Please read the instruction manual for the rf channel selector unit.**

The RF GRASP™ accessory consist of an RF gradient probe, an RF duplexer and an RF channel selector unit. The RF duplexer is used to direct proton RF power to either the gradient or the homogeneous coil in the probe, when using a single RF amplifier. Under normal operation, i.e. observing the NMR signal on the homogeneous RF coil, *RF OUT1* is connected to the preamp and *RF OUT2* is connected directly to the RF gradient connection of the probe. (If a second proton amplifier is used, its output is connected directly to the RF gradient connection of the probe and the RF duplexer is not needed.) A burndy cable connects the *DUPLEXER* burndy output on the RF channel selector with the duplexer and another burndy cable connects the *PROBE* burndy output on the RF channel selector with the probe. For probe tuning purposes the RF channel selector can be manually switched between the homogeneous channel (*CH1/CH3 HIGH*) and the gradient channel (*CH2/CH4 HIGH*).

Switching of the probe between the homogeneous and gradient RF channels is performed from the pulse program via **NMRword8 bit 7**. The following definitions are used:

```
#define HOM setnmr8^7
```

```
#define RFG setnmr8|7
```

These definitions are included in each pulse program or alternatively can be added to the *Avance.incl* file (see appendix).

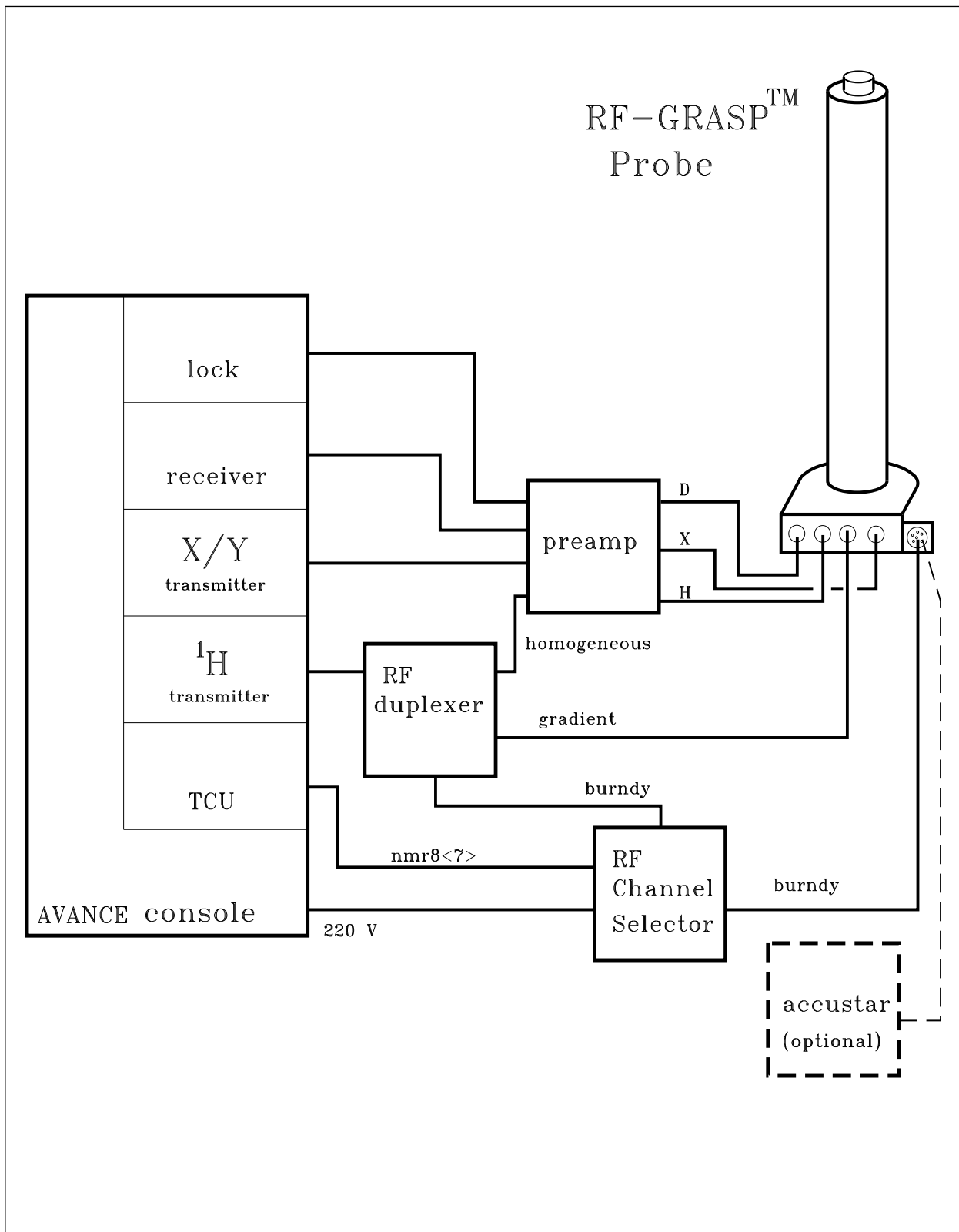
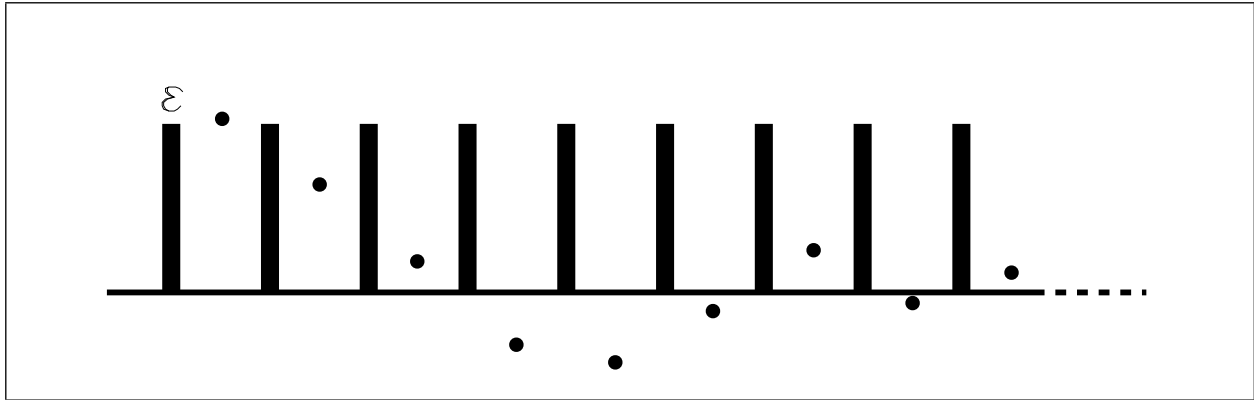


Figure 3 Set-up of the RF GRASP™ accessory.

## 6.2 Calibration of the RF Gradient



**Figure 4** *Pulse sequence of the 1D nutation experiment.*

RF field strengths can be calibrated by measuring the RF nutation frequency. Whereas in the case of a homogeneous coil the nutation frequency is simply determined from the length of a  $\pi/2$  pulse ( $\nu_{\text{rf}}=1/(4 \cdot P_{90})$ ), this is not possible for an RF gradient coil due to the distribution in field strength across the sample. In the latter case the gradient strength is obtained from a so-called nutation experiment, which registers the evolution of the magnetization under an RF field. A nutation experiment can be performed in a 2D fashion by acquiring Fid's as a function of increasing RF gradient pulse length, or in a 1D manner by acquiring datapoints during intervals in which the RF pulse is interrupted.

The 1D nutation sequence is easily used to calibrate the RF gradient strength. In this experiment the pulse length  $p2$  takes the place of the dwell time in a regular acquisition. An axis labeling in kHz is obtained by setting  $DW = p2 \cdot 1000$  (in  $\mu\text{s}$ ),  $FW=3e6$ ,  $AQMOD=QF$ . (Note that both excitation and receiving occur on the RF gradient channel, so in the set-up connect the RF for the gradient via the preamp to the probe!).

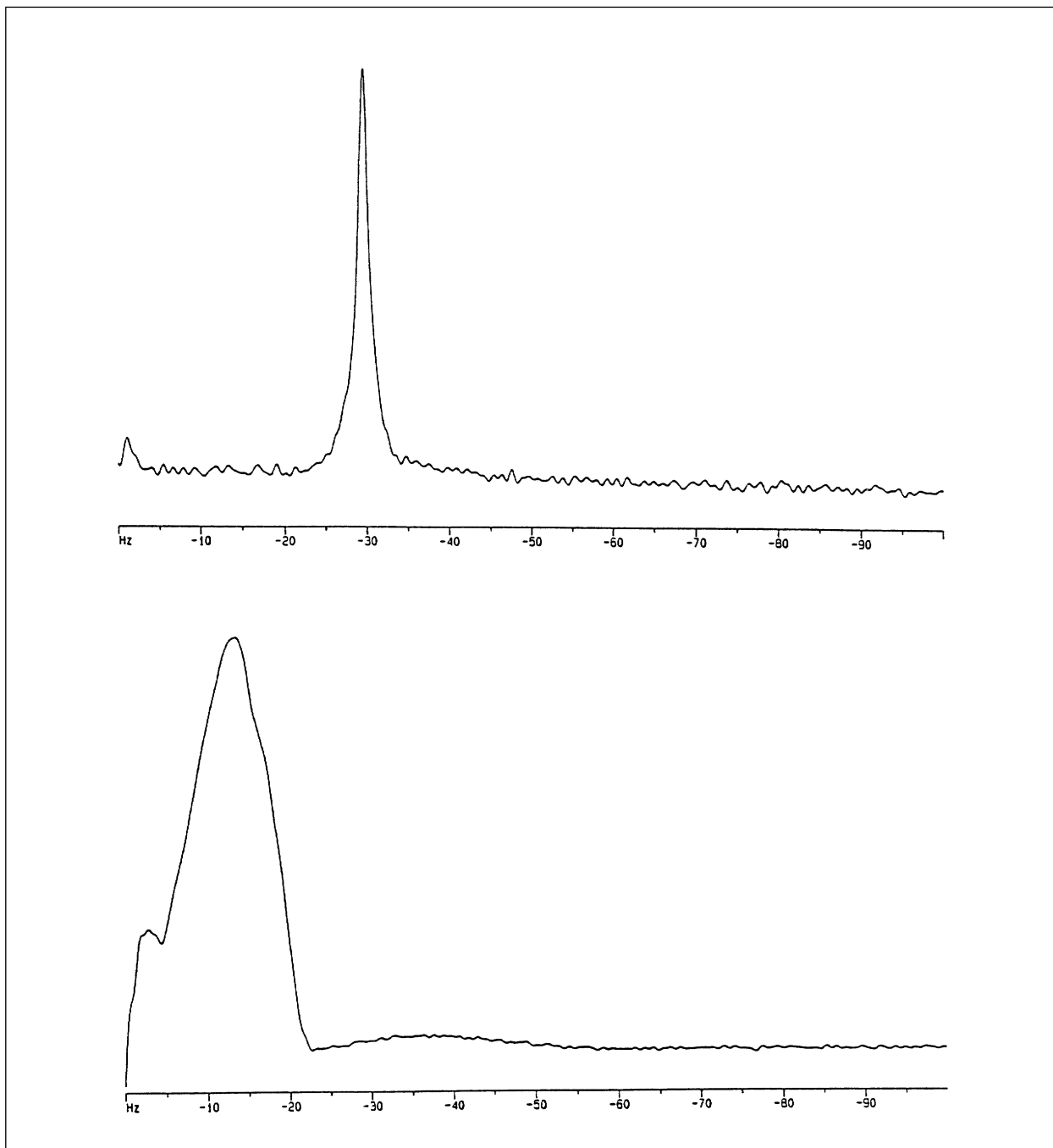


**Figure 5** Proton nutation spectra of a homogeneous RF coil (top) and a quadrupolar RF gradient coil (bottom).

### 6.3 P/N type Cosy selection

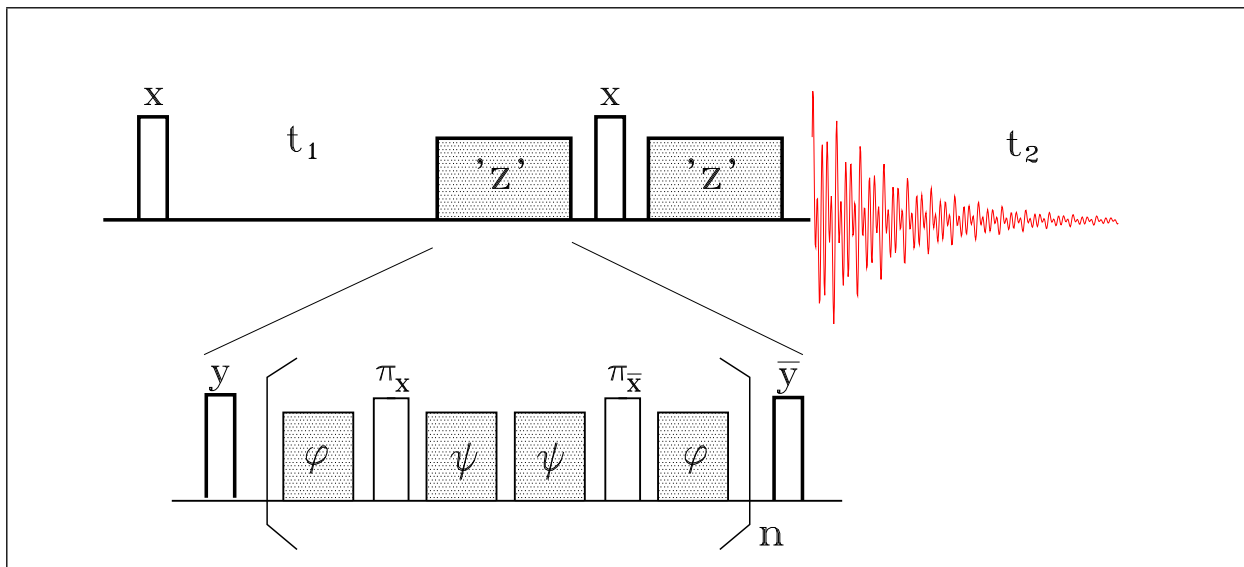


**Figure 6** Pulse sequence for the N-type selected COSY experiment.

The N-type selected COSY experiment (Figure 6) is performed in a single scan with RF gradients in composite z-rotations<sup>2</sup>. An effective z-rotation is achieved by sandwiching a planar gradient between two  $\pi/2$  pulses:  $\left(\frac{\pi}{2}\right)_y - G_x - \left(\frac{\pi}{2}\right)_{\bar{y}}$ . A planar gradient evolution is created with quadrupolar RF gradients, combined with  $\pi$  pulses in a conversion cycle. In the conversion cycle in the pulse sequence of Figure 6,  $\phi$  and  $\psi$  are chosen equal, resulting in an effective RF gradient  $G_x$ . The strength of the gradient is adjusted either by changing the length of the individual quadrupolar RF gradient pulses or by changing the number of repetitions of the conversion cycle.

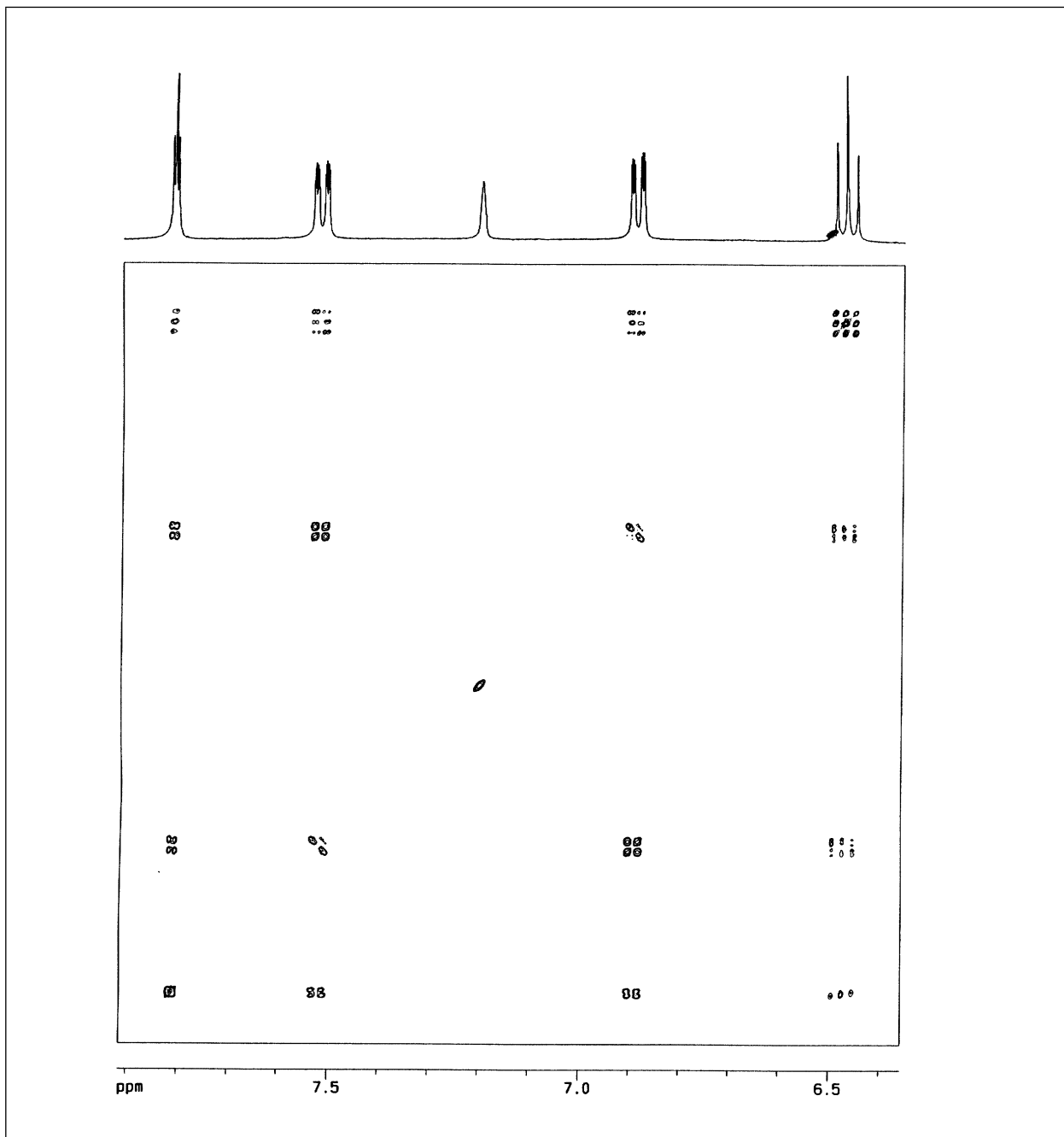


**Figure 7** *N*-type 400 MHz proton COSY spectrum of 1-chloro-3-nitrobenzene in deuterated benzene, represented in magnitude mode and obtained with a single scan per  $t_1$  increment. The gradient strength is 60 kHz/cm and the total duration of the gradient pulse is 4 m

## 6.4 Double Quantum filtered Cosy

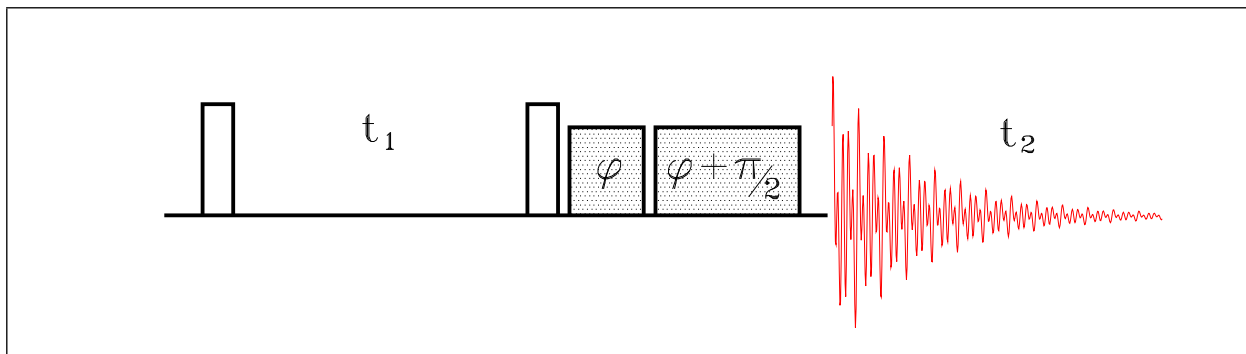


**Figure 8** *Pulse program of the RFG DQF COSY experiment with quadrupolar RF gradients.*

A version of a double quantum filtered Cosy experiment with RF gradients is depicted in Figure 8. This particular phase sensitive RFG DQF COSY experiment<sup>6</sup> is robust because the use of two 90 degree phase shifted gradients (ratio 1:2) renders it independent of the phase difference between the gradient and homogeneous RF. In samples in which a strong solvent signal may cause radiation damping, the probe is switched to the gradient mode during the evolution period  $t_1$ . This eliminates line broadening due to radiation damping in the first frequency domain and improves the suppression of the solvent signal by the double quantum filter.



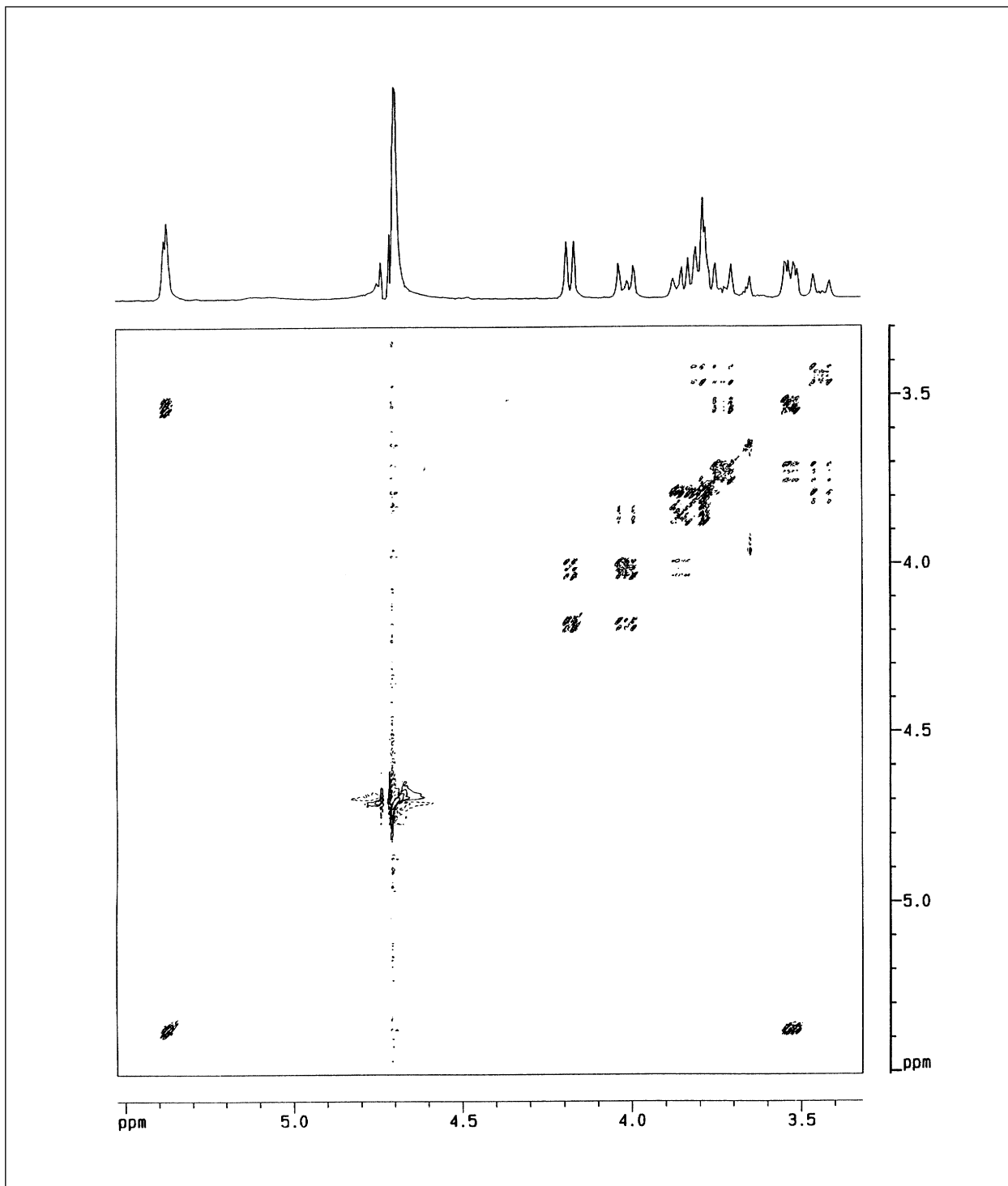


**Figure 9** 400 MHz proton phase sensitive RFG DQF COSY spectrum of sucrose in 90% H<sub>2</sub>O. The quadrupolar gradient pulse duration is 700 μs.

## 6.5 Solvent suppression with RF gradients

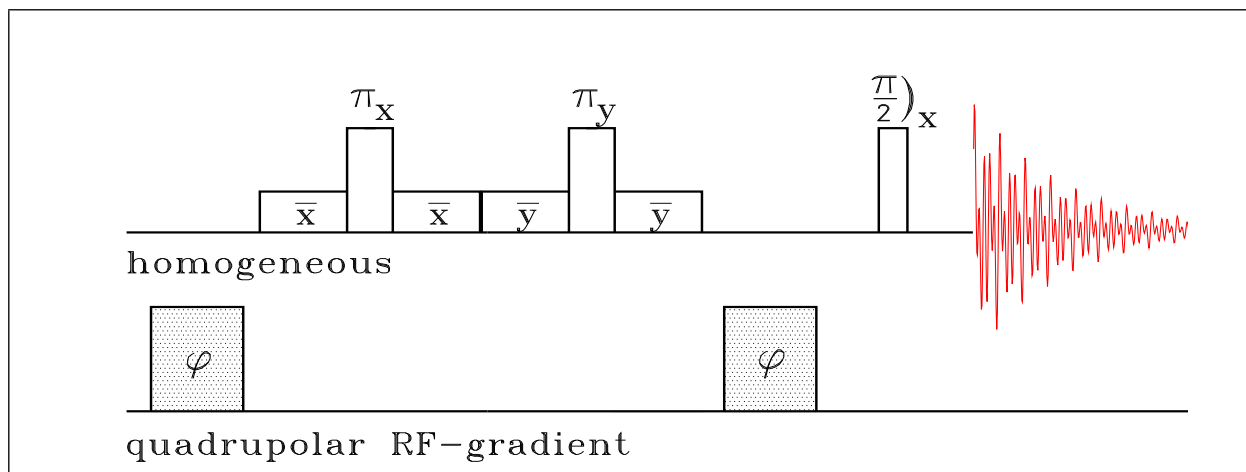


**Figure 10** *Pulse program of the RFG solvent suppression experiment with quadrupolar RF gradients.*

The dephasing of the magnetization due to an RF gradient pulse can be refocused by applying a  $\pi$  pulse to the spin system followed by a second gradient pulse of equal strength. An RF gradient spin echo sequence can be used for solvent suppression by making the inversion  $\pi$  pulse frequency selective, such that the solvent magnetization is not inverted and therefore is not refocused by the second gradient<sup>5</sup>. An example is shown in Figure 10, consisting of two quadrupolar RF gradient pulses and a frequency selective inversion sequence consisting of a hard  $\pi$  pulse sandwiched between two soft  $\pi/2$  pulses, selective for the solvent frequency. The inversion sequence is repeated with a 90 degree phase shift in order to recover the full signal intensity. The magnetization of spins other than the solvent spins, is refocused along the +z-axis and is observed following a  $\pi/2$  pulse.

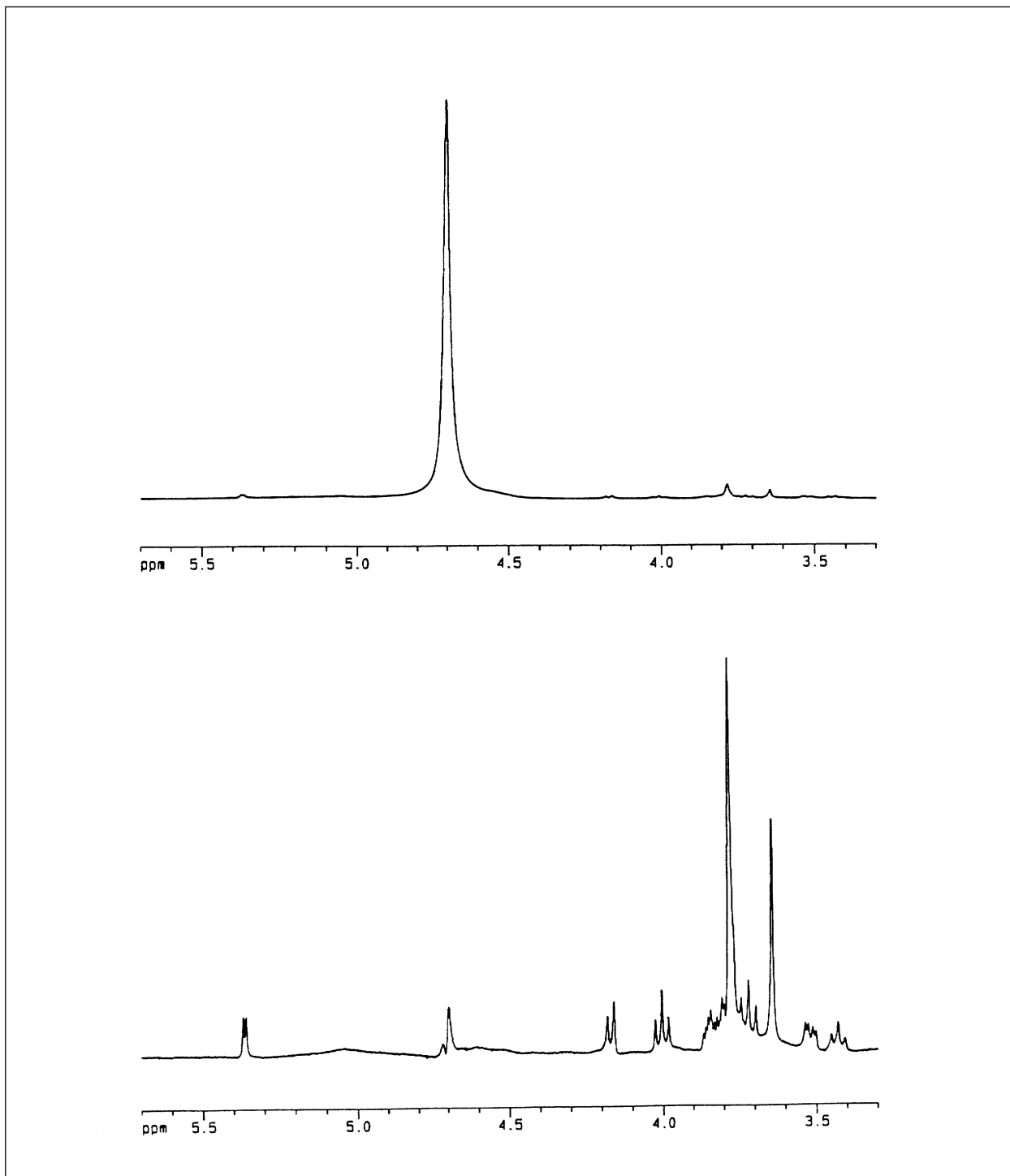


**Figure 11** *Single scan 400 MHz proton spectra of sucrose in water. The top spectrum is a single pulse spectrum and the bottom spectrum is obtained by suppressing the water resonance with quadrupolar RF gradients. The RF gradient pulse duration is 500  $\mu$ s and the selective pulse length is 2.78 ms.*

## 6.6 Heteronuclear Single Quantum Correlation

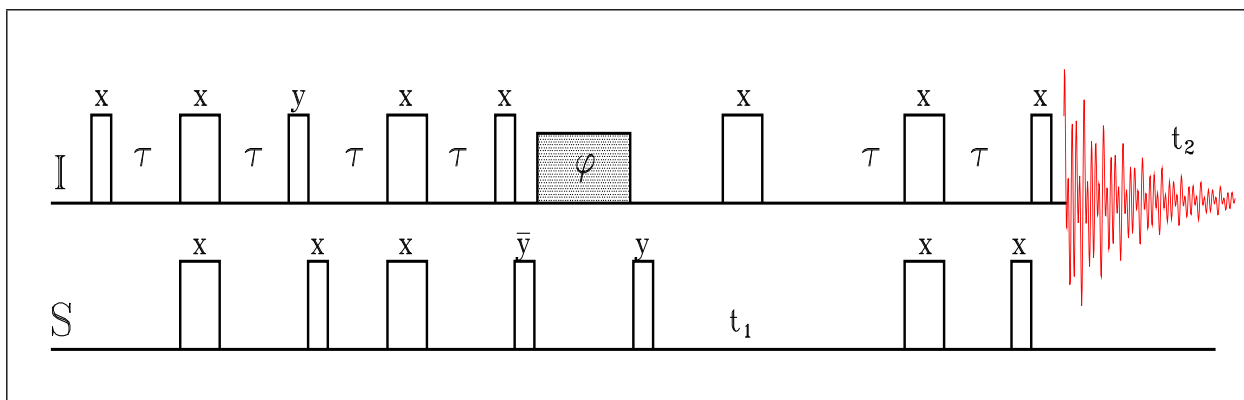


**Figure 12** Pulse program of an HSQC experiment with quadrupolar RF gradients.

RF gradients are frequency selective and in the **RF GRASP™** setup act only on proton spins. Heteronuclear coherences are, however, affected but only through the coupling to proton spins<sup>7,18</sup>. This situation therefore demands an experimental design which differs from a certain class of heteronuclear experiments in which the evolution under a  $B_0$  gradient of proton magnetization can be refocussed by a matched gradient when the coherence has a transverse heteronuclear component<sup>19</sup>.

An example of an RF gradient HSQC experiment involves longitudinal storage of the X-nucleus magnetization<sup>7</sup>. After the creation of antiphase S-magnetization via an INEPT sequence, the antiphase coherence is allowed to evolve into in-phase S-magnetization, which is subsequently stored along the main magnetic field. The magnetization of protons not coupled to a heteronucleus is pulsed back to the z-axis and dephased by a quadrupolar RF gradient pulse. The S-magnetization is returned to the transverse plane and evolves during  $t_1$  after which it evolves into an antiphase coherence which is returned to proton magnetization via the reverse INEPT step.

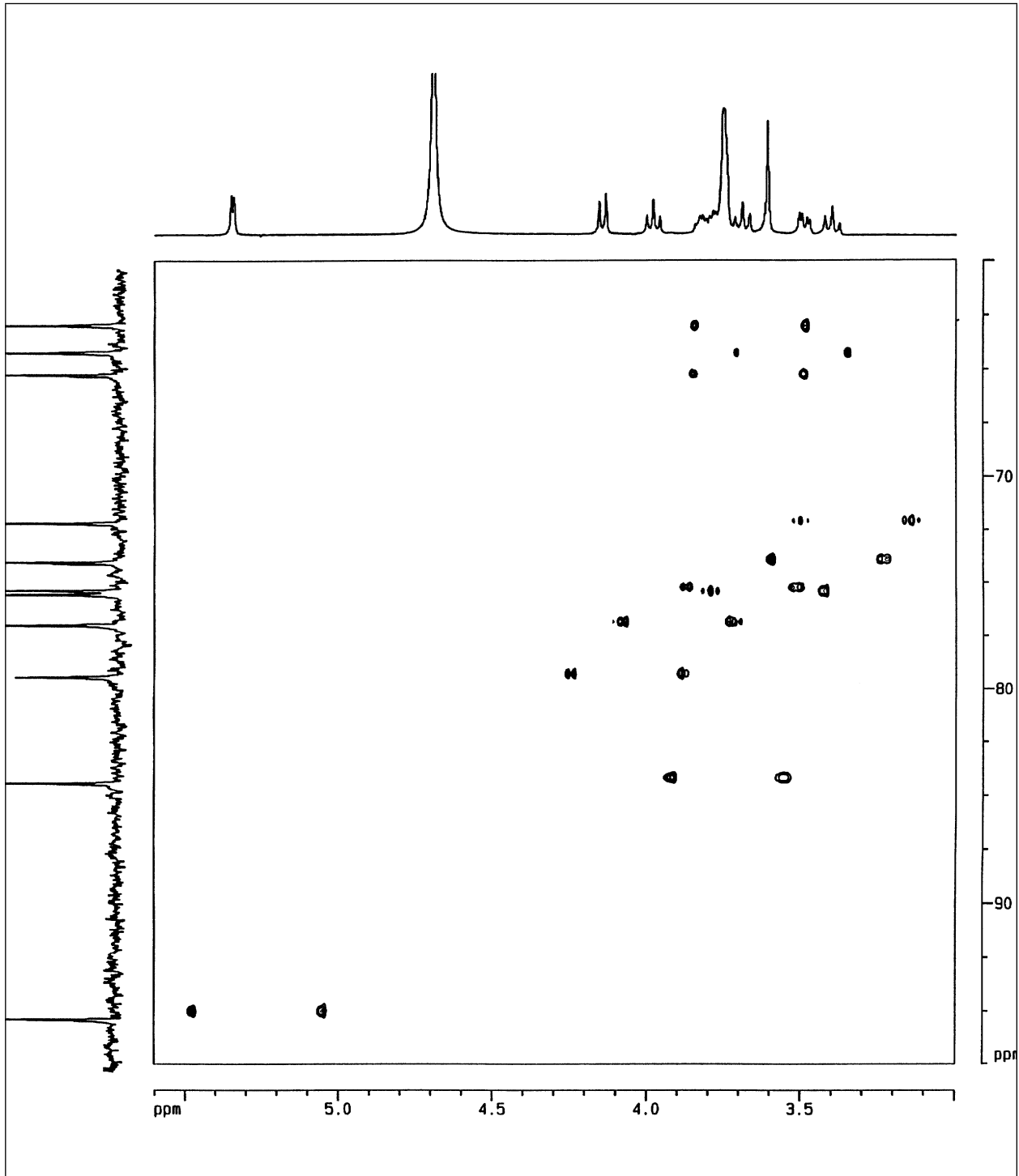


Figure 13 400 MHz  $^1\text{H}$ - $^{13}\text{C}$  HSQC experiment of sucrose in  $\text{D}_2\text{O}$ , employing longitudinal storage of the carbon magnetization while the uncoupled proton magnetization is dephased with a quadrupolar RF gradient pulse.

## 7 References

- [1] G. Estcourt, A.L. Davis, and J. Keeler. *J.Magn.Reson.* 96, 191, (1992).
- [2] W.E. Maas, F.H. Laukien, and D.G. Cory. *J.Magn.Reson.* A103, 115, (1993).
- [3] D. Canet, D. Boudot, A. Belmajdoub, A. Retournard, and J. Brondeau. *J.Magn.Reson.* 79, 168, (1988).
- [4] D.G. Cory, F.H. Laukien, and W.E. Maas. *Chem.Phys.Lett.* 212, 487, (1993).
- [5] W.E. Maas and D.G. Cory. *J.Magn.Reson.* A106, 256, (1994).
- [6] D.G. Cory, F.H. Laukien, and W.E. Maas. *J.Magn.Reson.* A105, 223, (1993).
- [7] W.E. Maas and D.G. Cory. *J.Magn.Reson.* A112, 229, (1995).
- [8] Y. Zhang, W.E. Maas, and D.G. Cory. *Molec. Phys.* 86, 347, (1995).
- [9] C.G. Anklin, M. Rindlisbacher, G. Otting, and F.H. Laukien. *J.Magn.Reson.* B106, 199, (1995).
- [10] W.E. Maas, F.H. Laukien, and D.G. Cory. *J.Magn.Reson.* A113, 274, (1995).
- [11] D. Canet, P. Tekely, N. Mahieu, and D. Boudot. *Chem.Phys.Lett.* 182, 541, (1991).
- [12] J. Brondeau, D. Boudot, P. Mutzenhardt, and D. Canet. *J.Magn.Reson.* 100, 611, (1992).
- [13] D. Canet, J. Brondeau, E. Mischler, and F. Humbert. *J.Magn.Reson.* A105, 239, (1993).
- [14] P. Mutzenhardt, J. Brondeau, and D. Canet. *J.Magn.Reson.* A108, 110, (1994).
- [15] J.J. Titman, A.L. Davis, E.D. Laue, and J. Keeler. *J.Magn.Reson.* 89, 176, (1990).
- [16] A.L. Davis, G. Estcourt, J. Keeler, E.D. Laue, and J.J. Titman. *J.Magn.Reson.* A105, 167, (1993).
- [17] C.D. Eads. *J.Magn.Reson.* A107, 109, (1994).
- [18] G. Otting and K. Wuthrich. *J.Magn.Reson.* 76, 569, (1988).
- [19] R.E. Hurd and B.K. John. *J.Magn.Reson.* 91, 648, (1991).

## 8 Appendix

### 8.1 Definitions for gradient switching

Add the following definitions to the preamble of the pulse programs for RF gradient spectroscopy or add these definitions to the **Avance.incl** file.

```
#define HOM setnmr8^7 ;switch to homogeneous channel
#define RFG setnmr8|7 ;switch to RF gradient channel
```

### 8.2 Gradient conversion cycle

```
;rfg.conv
;quadrupolar to planar gradient conversion cycle
;insert in pulse programs for planar gradient evolution

10    5u RFG
      p20:f1 ph20 ;RF gradient pulse phase phi
      5u HOM
      p3:f1 ph11 ;180 degree pulse phase x
      5u RFG
      p20:f1 ph21 ;RF gradient pulse phase psi
      5u
      p20:f1 ph21 ;RF gradient pulse phase psi
      5u HOM
      p3:f1 ph12 ;180 degree pulse phase -x
      5u RFG
      p20:f1:c4 ph20 ;RF gradient pulse phase phi
lo to 10 times ll
```

### 8.3 rfg.nutation

```
;rfg.nutation
;1D nutation sequence
;excitation and acquisition on RF gradient channel
#include <Avance.incl>
#define HOM setnmr8^7 ;switch to homogeneous channel
#define RFG setnmr8|7 ;switch to RF gradient channel
```

```
1    ze
2    d1 RFG ;switch to gradient mode
```

```

3      3u ph0 adc
      3u
      p2:f1 ph1      ;gradient pulse
      d2
      5u:x           ;acquire 1 datapoint
lo to 3 times l1    ;repeat l1 times; l1=td
rcyc=2 ph31
wr #0
5u HOM              ;switch back to homogeneous mode
exit

```

```

ph0=0
ph1=0
ph31=0

```

```

;p2 RF gradient pulse
;AQMOD=QF
;DW=p2*1000 (for axis labeling in kHz)
;FW=3e6

```

## 8.4 rfg.cosy

```

;rfg.cosy
;N-type COSY with RF gradients in composite z-rotation
;reference: W.E. Maas et al.
;      J. Magn.Reson. A103, 115, 1993

```

```

#include <Avance.incl>
#define HOM setnmr8^7      ;switch to homogeneous channel
#define RFG setnmr8|7     ;switch to RF gradient channel

```

```

1 ze
2      d1 HOM
3      p1:f1 ph1      ;90 degree pulse
d0
      p1:f1 ph10      ;start composite z-rotation

10     5u RFG          ;start gradient conversion cycle
      p20:f1 ph20     ;gradient pulse
      5u HOM
      p3:f1 ph11     ;180 degree pulse
      5u RFG

```



```

    p20:f1 ph21
    5u
    p20:f1 ph21
    5u HOM
    p3:f1 ph12
    5u RFG
    p20:f1 ph20      ;end gradient conversion cycle
    lo to 10 times l1
    5u HOM
    p1:f1 ph13      ;end composite z-rotation

p1:f1 ph2          ;cosy mixing pulse

    p1:f1 ph10      ;start composite z-rotation

11    5u RFG        ;start gradient conversion cycle
    p20:f1 ph20     ;gradient pulse
    5u HOM
    p3:f1 ph11      ;180 degree pulse
    5u RFG
    p20:f1 ph21
    5u
    p20:f1 ph21
    5u HOM
    p3:f1 ph12
    5u RFG
    p20:f1 ph20     ;end gradient conversion cycle
    lo to 11 times l1
    5u HOM
    p1:f1 ph13      ;end composite z-rotation
go=2 ph31
d1 wr #0 if #0 id0 zd
lo to 3 times td1
exit

ph1=0
ph2=0
ph10=0
ph11=2
ph12=1
ph13=3
ph20=0
ph21=0
ph31=0

;p1 : 90 degree pulse

```

```

;p3 : 180 degree pulse
;p20: RF gradient pulse
;d0 : incremented delay (2D)           [3 usec]
;d1 : relaxation delay; 1-5 * T1
;in0: 1/(1 * SW) = 2 * DW
;nd0: 1
;td1: number of experiments
;MC2: QF

```

## 8.5 rfg.dqfcosy

```

;rfg.dqfcosy
;DQF COSY with quadrupolar RF gradients
;phase sensitive using TPPI
;reference: D.G.Cory et al.
;      J. Magn.Reson. A105, 223, 1993

#include <Avance.incl>
#define HOM setnmr8^7      ;switch to homogeneous channel
#define RFG setnmr8|7     ;switch to RF gradient channel

1      ze
2      d1
3      p1:f1 ph1
;      5u RFG      ; optional switch to gradient channel
;      d0          ; to avoid radiation damping during t1
;      5u HOM
;      p1:f1 ph2
;      5u RFG
;      p20:f1 ph20
;      5u
;      p21:f1 ph21
;      5u HOM
go=2 ph31
d1 wr #0 if #0 id0 ip1 zd
lo to 3 times td1
exit

ph1=0
ph2=0
ph20=0
ph21=1
ph31=0

```

```

;p1 : 90 degree pulse
;p20: RF gradient pulse
;p21: RF gradient pulse=2*p21
;d0 : incremented delay (2D)           [3 usec]
;d1 : relaxation delay; 1-5 * T1
;in0: 1/(2 * SW) = DW
;nd0: 1
;td1: number of experiments
;MC2: TPPI

```

## 8.6 rfg.watersup

```

;rfg.watersup
;Water suppression with quadrupolar RF gradients
;reference: W.E. Maas et al.
;      J. Magn.Reson. A106, 256, 1994

#include <Avance.incl>
#define HOM setnmr8^7      ;switch to homogeneous channel
#define RFG setnmr8|7     ;switch to RF gradient channel

1      ze
2      d1
      5u RFG
      p20:f1 ph20         ;first RF gradient pulse

      5u HOM              ;selective 180)x pulse
      p10 pl2:f1 ph10:r   ;      selective pulse power pl2
      p3:f1 ph11          ;      180 degree hard pulse
      p10 pl2:f1 ph10:r   ;      selective pulse power pl2

                        ;selective 180)y pulse
      p10 pl2:f1 ph12:r   ;
      p3:f1 ph13          ; (see above)
      p10 pl2:f1 ph12:r   ;

      5u RFG
      p20:f1 ph20         ;second RF gradient pulse
      5u HOM
      p1:f1 ph1           ;readout pulse
go=2 ph31
d1 wr #0 if #0 id0 ip1 zd
lo to 3 times td1
exit

```

```

ph1=0
ph10=0
ph11=2
ph12=1
ph13=3
ph20=0
ph31=0

```

```

;p1 : 90 degree pulse
;p3 : 180 degree pulse
;p10: selective 90 degree pulse
;p20: RF gradient pulse
; adjust phases ph10 and ph12 with phcor10 and phcor12 to be
; exactly opposite to ph11 and ph13

```

## 8.7 rfg.hsqc

```

;rfg.hsqc
;1H-X HSQC with quadrupolar RF gradients
;phase sensitive using TPPI
;reference: W.E. Maas et al.
;      J. Magn.Reson. A112, 229, 1995

#include <Avance.incl>
#define HOM setnmr8^7 ;switch to homogeneous channel
#define RFG setnmr8|7 ;switch to RF gradient channel

1      ze
2      d1
3      (p1 ph1):f1
        d4
        (p3 ph2):f1 (p13 ph10):f2
        d4
        (p1 ph3):f1 (p11 ph11):f2
        d4
        (p3 ph2):f1 (p13 ph10):f2
        d4
        (p1 ph4):f1 (p11 ph12):f2
        5u RFG
        (p20 ph20):f1
        5u HOM
        (p11 ph13):f2
        d0
        (p3 ph2):f1

```

```

d0
d4
(p3 ph2):f1 (p13 ph11):f2
d4
(p1 ph4):f1 (p11 ph11):f2
go=2 ph31
d1 wr #0 if #0 id0 ip13 zd
lo to 3 times td1
exit

```

```

ph1=0
ph2=0
ph3=1
ph4=0
ph10=0
ph11=0
ph12=3
ph13=1 3
ph20=0
ph31=0 2

```

```

;p1 : proton 90 degree pulse
;p3 : proton 180 degree pulse
;p11: X 90 degree pulse
;p13: X 180 degree pulse
;p20: RF gradient pulse
;d0 : incremented delay (2D)           [3 usec]
;d1 : relaxation delay; 1-5 * T1
;d4 : 1/(4J)XH
;in0: 1/(4 * SW_X) = 1/2* DW_X
;nd0: 4
;td1: number of experiments
;MC2: TPPI

```